ELSEVIER

Journal of Photochemistry and Photobiology A: Chemistry 103 (1997) 105–113

Journal of PHOTOCHEMISTRY AND PHOTOBIOLOGY A:CHEMISTRY

# Low-temperature photochemistry of nitro-substituted aromatic azides; subsequent reactions of intermediates

T. Harder [a], R. Stößer [b], P. Wessig [a], J. Bendig [a,*]

[a] *Institute of Chemistry, Organic and Bioorganic Chemistry, Humboldt University Berlin, Hessische Str. 1-2, 10115 Berlin, Germany*

[b] *Institute of Chemistry, Physical and Theoretical Chemistry, Humboldt University Berlin, Hessische Str. 1-2, 10115 Berlin, Germany*

Received 29 January 1996; accepted 1 October 1996

**Abstract**

Triplet 4-nitrophenylnitrene (**1B**) and triplet 4-nitrene-4′-nitrostilbene (**2B**) are characterized by their low-temperature UV-Vis and ESR spectra as well as by their consecutive thermal and photochemical reactions. The main thermal reaction of **1B** and **2B** between 77 and 90 K is a stepwise, twofold hydrogen abstraction from the methyltetrahydrofuran (2-MTHF) matrix solvent, leading to the corresponding primary amines. The activation energy of the first hydrogen abstraction of **1B** and **2B** is not influenced by their structure and is about 30 kJ mol$^{-1}$. A similar amount of energy is required for the second hydrogen abstraction. Since the activation energy required for diffusion in a solid 2-MTHF matrix is about 87 kJ mol$^{-1}$, bimolecular processes that require diffusion are less efficient between 77 and 87 K. While **2B** is photochemically stable, **1B** reacts after optical excitation under hydrogen abstraction from the solvent to form an imino radical **1C**. The photochemically induced hydrogen abstraction after the excitation of **1B** and the absence of the analogous reaction after the excitation of **2B** can be explained by means of two models; either as a hot ground state reaction or as a reaction starting from an electronically excited state of **1B**. In the latter model, it is assumed that the activation energy of the hydrogen abstraction is lower in the first excited state than in the electronic ground state of **1B**. Both models predict that the hydrogen abstraction is more efficient if the difference in energy between the electronic ground and electronically excited states is high enough. This is the case in **1B** but not in **2B**.

The experimental results are discussed in connection with theoretical statements arising from quantum chemical calculations.

*Keywords:* Aromatic azides; 4-Azido-4′-nitrostilbene; Excited intermediates; Low-temperature photochemistry; 4-Nitrophenylnitrene; Photolysis

## 1. Introduction

Singlet phenylnitrene is the primary product after the photolysis of phenylazide; above 165 K it reacts thermally to form didehydroazepine, while it mainly converts into triplet phenylnitrene by an isc process at low temperatures ($T < 165$ K) [1]. It was shown by the IR and ESR results of Chapman and Le Roux that triplet phenylnitrene reacts after optical excitation at 8 K to form didehydroazepine, too [2]. This mechanism was confirmed independently by Hayes and Sheridan on the basis of UV-Vis and IR investigations at 12 K in nitrogen matrices [3].

The nitro-substituted aromatic azides are of special interest since they are often used as photolabelling agents [5]. For this reason, their reactions have been investigated intensively in the past. Both the transient absorption spectra and theanalysis of products provide evidence that the photolysis of 4-nitrophenylazide (**1A**) at 300 K leads to the formation of triplet 4-nitrophenylnitrene ($\lambda_{max} = 380$ nm) which dimerizes to form 4,4′-dinitroazobenzene [6] or it abstracts hydrogen from the solvent, yielding 4-nitroaniline [4]. Efimov et al. studied the photochemistry of 4-nitrophenylazide in ethanol at 77 K. In contrast to Liang et al. [6], a UV-Vis absorption band at 312 nm was assigned to triplet 4-nitrophenylnitrene [7,8]. On the other hand, Dunkin et al. found that 5-nitro-1,2-didehydroazepine is obtained after the photolysis of **1A** in an argon matrix at 8 K [9].

Although the photochemistry of 4-nitrophenylazide is still under contradictory discussion, nothing is known about the primary products obtained after the optical excitation of aromatic azides that have larger conjugated $\pi$-systems (e.g. 4-azido-4′-nitrostilbene). Our preliminary examinations have shown that the subsequent reactions of "larger" nitrenes differ from those of phenylnitrene derivatives.

* Corresponding author. Tel.: +49 30 20937274; fax.: +49 30 20937274.


*PII* S1010-6030(96)04516-9

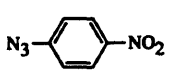


1A

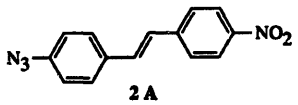


2A

In this report, an analysis of the photochemistry of 4-nitrophenylazide (**1A**) and 4-azido-4′-nitrostilbene (**2A**) at 77 K is presented with regard to the following aspects: firstly, to clarify the number and structure of products which appear after the photolysis of **1A** and **2A**, the sequence of their formation, and their spectroscopic properties; secondly, to collect information about the type of the main consecutive thermal and photochemical reactions of the primary products; thirdly, to discuss kinetic aspects of the stepwise thermal hydrogen abstraction of the two nitrenes; and, finally, to explain the observed differences in the consecutive photochemical reactions of the two investigated nitrenes on the basis of their chemical structure.

The intermediates were characterized by UV-Vis spectral studies in combination with ESR studies, as well as by their chemical reactions between 77 and 300 K.

Quantum chemical calculations are used to understand the experimental findings.

## 2. Experimental

The UV-Vis spectra were recorded on a Hitachi U-3410 double-beam spectrophotometer, using a 1 mm quartz cell. The temperature could be regulated and kept constant between 77 and 300 K with a precision of 0.1 K, using a cryostat equipped with a temperature controller. The ESR spectra were measured using an ERS-300 spectrometer (X-band microwave unit; 100 kHz field modulation; $f=9.18$ GHz) equipped with an optical transmission cavity. The sample was placed in a quartz tube (3 mm o.d.) and cooled within the cavity using a liquid nitrogen Dewar insert. For both the UV-Vis and the ESR experiments, the samples were irradiated through a water cell (10 cm) and a metal interference filter (313 or 365 nm) using a high-pressure mercury lamp (500 W). For the UV-Vis experiments, additional glass filters were used to reduce the light intensity. Reference experiments confirmed the compatibility of the time-scales of product formation (ratio of photolysis) observed by UV-Vis and ESR spectroscopy. HPLC investigations were carried out using an RP 18 column, employing a mobile phase comprising methanol–water mixtures of different compositions and a UV-Vis diode array detector (Kontron, DAD 440).

The chemicals were used as purchased from the Aldrich Chemical Company. 2-Methyltetrahydrofuran (2-MTHF) was distilled from calcium hydride. All syntheses were carried out under yellow light. 4-Nitrophenylazide (**1A**) was synthesized using a standard procedure starting from 4-nitroaniline [16]. The *trans*-4-azido-4′-nitrostilbene (**2A**) was synthesized as described previously, starting with the diazotization of *trans*-4-amino-4′-nitrostilbene followed by treatment with sodium azide at −10°C [10].

The absolute amount of the final products **1E**, **1F** and **2C** is very small (about $10^{-7}$–$10^{-8}$ mol). For this reason, they could only be characterized using HPLC. Species **1E** and **2C** were identified by comparing their retention times and UV-Vis spectra with those of authentic samples. No reference substance was available to identify **1F**. The characteristics of **1F** (UV-Vis spectrum and the polarity arising from the HPLC retention time) are very similar to those of secondary amines such as 4-methylamino-4′-nitrobenzene or 4-dimethylamino-4′-nitrobenzene.

The zfs parameters of nitrenes were determined by simulation of their experimental ESR spectra using the full diagonalization of an appropriate spin-hamiltonian matrix ($s=1$) [10].

## 3. Results and discussion

### 3.1. Low-temperature photochemistry of 4-nitrophenylazide (1A) and subsequent reactions

The primary reactions of 4-nitrophenylazide (**1A**) as well as the consecutive thermal and photochemical reactions of triplet 4-nitrophenylnitrene (**1B**) between 77 and 90 K are summarized below. 4-Nitrophenylazide (**1A**) reacts photochemically to form triplet 4-nitrophenylnitrene (**1B**). After excitation, **1B** abstracts a single hydrogen atom from the solvent to form an imino radical (**1C**). This further reacts thermally to form 4-nitroaniline (**1E**). In a side reaction, **1B** reacts photochemically to produce a small amount of species **1D**. On the other hand, triplet 4-nitrophenylnitrene (**1B**) reacts thermally between 77 and 90 K under twofold hydrogen abstraction from the solvent, forming 4-nitroaniline (**1E**) also. Furthermore, a small amount of a secondary amine **1F** is formed by the combination of **1C** with a solvent radical. The coupling of two nitrenes to form 4,4′-dinitroazobenzene is prevented by the high viscosity of the 2-MTHF matrix [14] between 77 and 90 K.

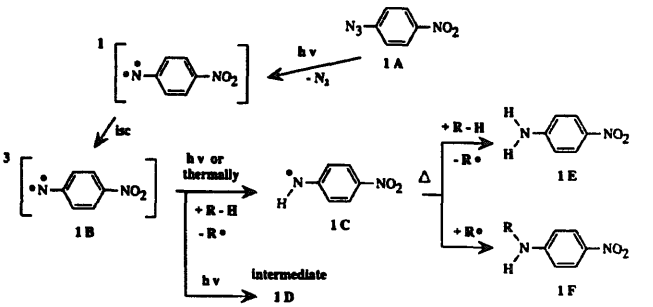


The mechanism proposed is a result of UV-Vis and ESR spectroscopic investigations as well as of product analysis after thawing out the matrix.

The irradiation ($\lambda_{exc}=313$ nm) of 4-nitrophenylazide (**1A**) in 2-MTHF at 77 K leads to a decrease in the absorbance of the azide ($\lambda_{max}=326$ nm). Subsequently, the absorption band of species **1B** ($\lambda_{max}=312$ nm) appears, which is blue-

shifted relative to the absorption spectrum of **1A** (Fig. 1a). The reaction is uniform within the initial period of photolysis, which is demonstrated by an isosbestic point at 362 nm as well as by the linear $\Delta E$ diagram (inset in Fig. 1a). Further irradiation ($\lambda_{exc} = 313$ nm) causes a decrease in the absorbance of **1B** and an increase in the absorbance of species **1C** ($\lambda_{max} = 382$ nm; Fig. 1a,b). Beside **1C**, another transient **1D** ($\lambda_{max} = 462$ nm) is produced during the excitation of **1B**. The photochemical reaction of **1B** to form **1C** and **1D** is spectroscopically uniform in the final period of photolysis when **1A** is completely decomposed. This is indicated by the isosbestic points at 270 and 335 nm and by the $\Delta E$ diagram which is shown in the inset of Fig. 1b. During the transition period, when **1A** reacts to form **1B** and **1B** itself reacts at the same time to produce **1C** and **1D**, the photochemical reaction is not uniform. This is demonstrated by the non-linear parts in the $\Delta E$ diagrams of the final period of photolysis shown in Fig. 1a and of the initial period of photolysis shown in Fig. 1b.

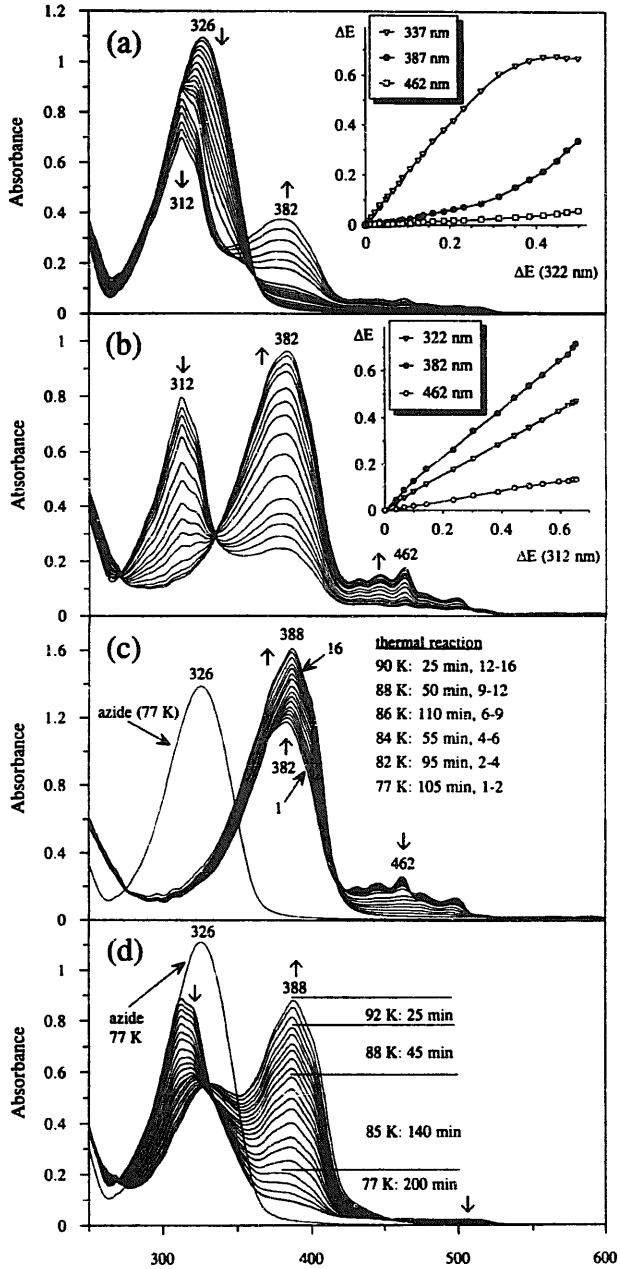


Fig. 1. (a) UV-Vis irradiation spectra of 4-nitrophenylazide (**1A**) at 77 K in 2-MTHF ($\lambda_{exc} = 313$ nm) and the corresponding $\Delta E$ diagram. (b) UV-Vis irradiation spectra of triplet 4-nitrophenylnitrene (**1B**) obtained after prolonged irradiation of the sample shown in (a) at 77 K in 2-MTHF ($\lambda_{exc} = 313$ nm) and the corresponding $\Delta E$ diagram. (c) UV-Vis spectra obtained during the thermal reaction of the imino radical (**1C**) and **1D** between 77 and 90 K in 2-MTHF. (d) UV-Vis spectra obtained during the thermal reaction of triplet 4-nitrophenylnitrene (**1B**) between 77 and 92 K in 2-MTHF.

The UV-Vis spectra obtained during the thermal reactions of **1C** and **1D** are shown in Fig. 1c. Species **1C** reacts thermally between 77 and 90 K to produce 4-nitroaniline (**1E**; $\lambda_{max}$(77 K) = 388 nm; identified by product analysis and by the strong similarity of the UV-Vis spectra of an authentic sample of 4-nitroaniline and **1E** between 77 and 300 K). During the thermal reaction of **1D** ($\lambda_{max} = 462$ nm), two steps are distinguishable. Between 77 and 86 K, **1D** reacts to form a further species absorbing at $\lambda_{max} = 474$ and 500 nm (isosbestic points at 468, 520 and 600 nm). Above 87 K, this additional intermediate reacts thermally, which is indicated by an overall decrease in the absorbance above 425 nm. Product analysis at 300 K provides evidence for two products, mainly **1E** and a small amount of a by-product **1F**. On the basis of the arguments given in the experimental section, **1F** is assumed to be a secondary amine which is formed by a pseudo insertion of the triplet nitrene into a C–H bond of the solvent [12]. Since the primary reactions of **1B** are the main topic of this chapter, the characteristics of **1F** were not investigated in detail. No additional product was found that could be related to the precursor **1D**. This is probably due to the small concentration ($c < 5 \times 10^{-6}$ mol $l^{-1}$) of **1D** formed under the given conditions.

A sample of 4-nitrophenylazide was photolyzed partially in order to decompose only 50% of **1A**. In this way, only **1B** and not **1C** and **1D** are produced in detectable concentrations (Fig. 1d). This allows information to be collected about the thermal reaction of **1B**. During the thermal reaction of **1B** between 77 and 90 K, 4-nitroaniline (**1E**) is finally formed. This is indicated by an increase in the absorbance at $\lambda_{max} =$ 388 nm (Fig. 1d). The analysis of the products at 300 K confirms the formation of mainly 4-nitroaniline (**1E**; $\lambda_{max}$(methanol) = 378 nm; 300 K) and of a small amount of **1F** ($\lambda_{max}$(methanol) = 376 nm; 300 K).

Additional significant results arise from the corresponding ESR investigations. At the same time, when the UV-Vis spectrum of **1A** is replaced by that of **1B**, an increase in the absorbance of a triplet mononitrene signal ($H_{x,y} = 668.7$ mT) is monitored in the ESR spectrum. On the basis of the calculated zfs parameter ($|D/hc| = 0.987$ cm$^{-1}$) in comparison with that of triplet phenylnitrene (see (b) in Ref. [2]), this signal is assigned to triplet 4-nitrophenylnitrene (**1B**). During further photolysis ($\lambda_{exc} = 313$ nm), the triplet signal of **1B** disappears. At the same time, an ESR signal in the 330 mT region increases in intensity (Fig. 2 (white points), and Fig. 3). Following Refs. [11,12], this signal is assigned to a

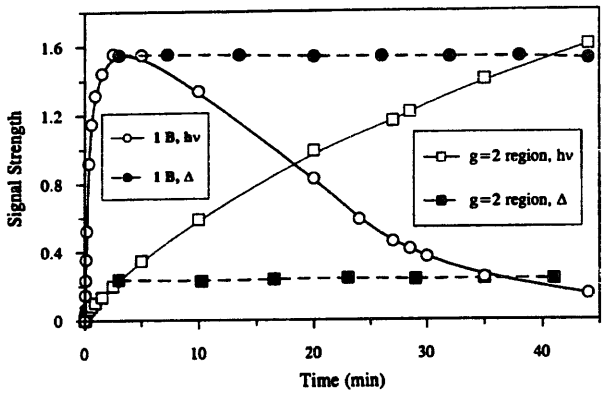


Fig. 2. Relative concentrations (ESR determination) of triplet 4-nitrophenylnitrene (**1B**) and the imino radical (**1C**) as a function of the irradiation time (white points; $\lambda_{exc}=313$ nm) and of the dark reaction time at 77 K in 2-MTHF (black points). The latter functions were monitored after photolyzing **1A** for only 3 min ($\lambda_{exc}=313$ nm) to obtain a high stationary concentration of **1B**. The concentrations of **1B** and **1C** were measured in the dark at 77 K as a function of time.

radical pair which consists of an imino radical and a radical of 2-MTHF.

The thermal reaction of **1B** at 77 K was also followed by ESR spectroscopy. For this reason, a sample of **1A** was photolyzed for only 3 min in order to obtain a high stationary concentration of **1B**. As shown in Fig. 2 (black points) the thermal reaction at 77 K causes only a very small decrease in the concentration of **1B** and a very small increase in the concentration of **1C** (indicated by the absorbance of the radical pair at 330 mT). This was also found from the UV-Vis investigations (Fig. 1d).

Comparison of the UV-Vis results with the ESR results shows that **1B** is triplet 4-nitro-phenylnitrene ($\lambda_{max}=312$ nm; $|D/hc|=0.987$ cm$^{-1}$). In addition, the assignment of the UV-Vis spectrum of **1B** is supported by chemical arguments since the species absorbing at 312 nm reacts to form 4-nitroaniline ($\lambda_{max}=388$ nm). It must, therefore, be the triplet nitrene **1B**. Since hydrogen abstraction is a typical reaction of triplet species, this implies that **1B** exists at 77 K mainly in the triplet state. The UV-Vis spectrum of **1B** can therefore be described by $T_1 \rightarrow T_n$ transitions.

On the basis of two arguments, **1C** is assigned to the imino radical. Firstly, the ESR signal in the 330 mT region is very similar to that reported in Refs. [11,12]. The latter signal was found to be typical for radical pairs. The second argument is more significant and arises from mechanistic aspects. Since **1C** is the only transient between the triplet nitrene **1B** and 4-nitroaniline (**1E**), it can only be an imino radical.

The investigations clearly indicate that **1D** is produced photochemically from **1B**. Besides the hydrogen abstraction, triplet phenylnitrenes are only known to undergo at 77 K a photochemically induced ring expansion to form didehydroazepines [2,9,11–13]. Thus, the absorption band at 462 nm should most probably be due to 5-nitro-1,2-didehydroazepine. However, there is no similarity between the UV-Vis spectrum of **1D** and that of the didehydroazepine produced after the optical excitation of triplet phenylnitrene [13]. Because of this discrepancy, we are investigating the nature of **1D**, which we will report on shortly.

### 3.2. *Low-temperature photochemistry of trans-4-azido-4'-nitrostilbene (2A) and subsequent reactions*

The primary reactions of 4-azido-4'-nitrostilbene (**2A**) and the subsequent reactions of transients between 77 and 90 K are summarized in the following scheme.

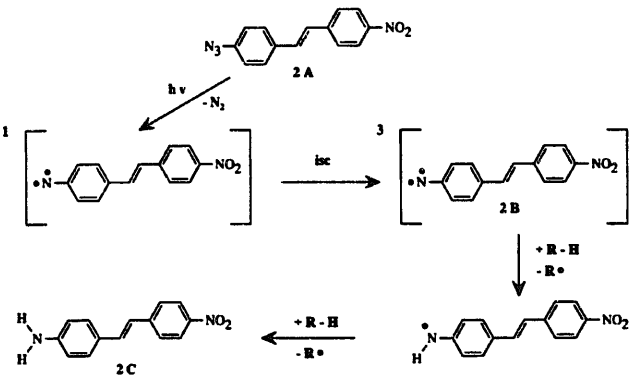


The mechanism is arrived at from UV-Vis and ESR spectroscopic findings and it results from the following chemical arguments.

During the irradiation ($\lambda_{exc}=365$ nm) of 4-azido-4'-nitrostilbene (**2A**; $\lambda_{max}=389$ nm) in 2-MTHF at 77 K, the absorption band of the azide is replaced by that of only one UV-Vis-active species (**2B**) which absorbs in the same spectral region ($\lambda_{max}=380$, 395, 450 nm) as the starting compound. The $\Delta E$ diagram indicates the photochemical reaction to be uniform (inset in Fig. 4a). Prolonged irradiation ($\lambda_{exc}=365$ nm) shows that **2B** is photochemically stable (Fig. 5), whereas triplet 4-nitrophenylnitrene (**1B**) is unstable after excitation.

The thermal reaction of **2B** between 77 and 90 K leads to the formation of species **2C** ($\lambda_{max}$(77 K in 2-MTHF) = 461 nm; Fig. 4b). Species **2C** is thermally stable up to 300 K. The UV-Vis spectrum of **2C** is reversibly blue-shifted

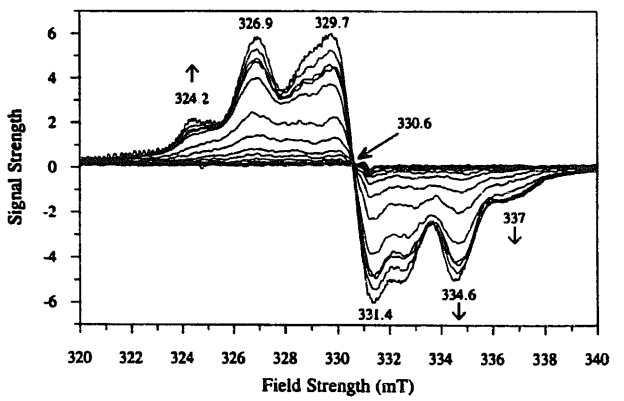


Fig. 3. ESR spectra of the radical pair consisting of **1C** and a 2-MTHF radical; obtained after the irradiation of 4-nitrophenylazide (**1A**) in 2-MTHF at 77 K.

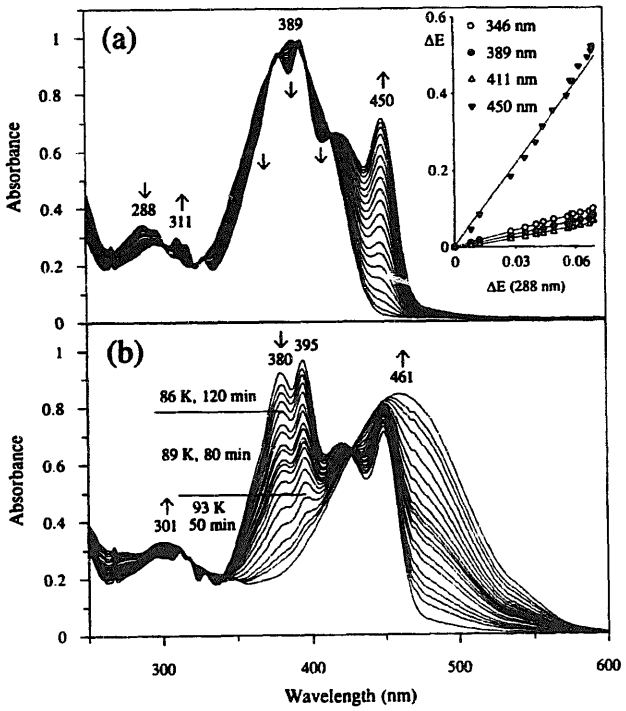


Fig. 4. (a) UV-Vis irradiation spectra of 4-azido-4′-nitrostilbene (**2A**) at 77 K in 2-MTHF ($\lambda_{exc}$ = 365 nm) and the corresponding $\Delta E$ diagram. (b) UV-Vis spectra of the thermal reaction of triplet 4-nitrene-4′-nitrostilbene (**2B**) between 77 and 90 K in 2-MTHF.

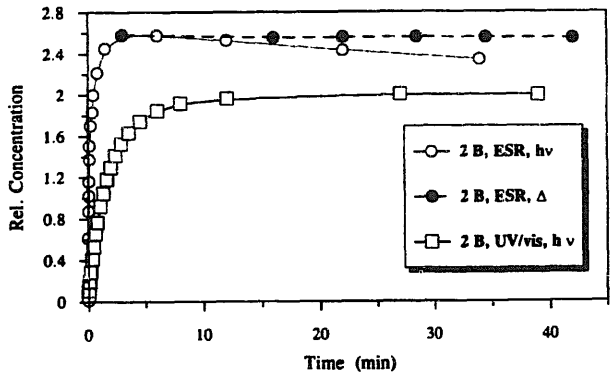


Fig. 5. Relative concentration of triplet 4-nitrene-4′-nitrostilbene (**2B**) as a function of the irradiation time and dark reaction time, determined by ESR and UV-Vis spectroscopy at 77 K in 2-MTHF.

with increasing temperature. The product analysis shows that **2C** is 4-amino-4′-nitrostilbene ($\lambda_{max}$(methanol, 300 K) = 403 nm). The formation of secondary amines was not observed.

Mechanistic arguments suggest that **2B** is triplet 4-nitrene-4′-nitrostilbene (final UV-Vis spectrum in Fig. 4a) which reacts (as **1B**) thermally under twofold hydrogen abstraction from the solvent.

The ESR investigations confirm that triplet 4-nitrene-4′-nitrostilbene (**2B**; $H_{x,y}$ = 620.8 mT; $|D/hc|$ = 0.801 cm$^{-1}$) is formed efficiently whereas only traces of radicals are produced during irradiation ($\lambda_{exc}$ = 365 nm). On prolonged irradiation with $\lambda_{exc}$ = 365 nm, the signal intensity of the triplet nitrene decreases very slowly (Fig. 5). This small effect can mainly be described by a warming up of the matrix caused by the irradiation source [10]. During the dark reaction at 77 K, the signal intensity of the triplet nitrene **2B** remains nearly constant (Fig. 5). This is in agreement with the results of the UV-Vis spectroscopic investigations of **2B**.

### *3.3. Kinetic aspects of the stepwise thermal hydrogen abstraction by the nitrenes 1B and 2B*

Aromatic nitrenes are known to form amines thermally but nothing has been reported on the observation of the imino radical intermediate. We therefore investigated the kinetics of the two steps of the thermal hydrogen abstraction of **1B** and **2B**.

Since there is a considerable surplus of solvent molecules, diffusion should be negligible during the hydrogen abstraction of the nitrene from the solvent. This reaction can therefore be described as a pseudo-first-order process. The pseudo-first-order rate constants ($k_1'$) for the disappearance of triplet 4-nitrophenylnitrene (**1B**) and triplet 4-nitrene-4′-nitrostilbene (**2B**) are summarized in Table 1. The evaluation of these values according to the Arrhenius equation is shown in Fig. 6. The average activation energy, required for the first hydrogen abstraction, is estimated from the slopes of the plots and amounts to 30.3 kJ mol$^{-1}$ (±3.5 kJ mol$^{-1}$) for the triplet 4-nitrophenylnitrene (**1B**) and to 32.5 kJ mol$^{-1}$ (±7 kJ mol$^{-1}$) for the triplet 4-nitrene-4′-nitrostilbene (**2B**).

In general, the concentration of the imino radical during thermal twofold hydrogen abstraction of a nitrene is deter-

Table 1
Pseudo-first-order rate constants $k_1'$ (min$^{-1}$)[a] for the first step of hydrogen abstraction by triplet 4-nitrophenylnitrene (**1B**) and triplet 4-nitrene-4′-nitrostilbene (**2B**)

| Temperature (K) | Triplet 4-nitrophenylnitrene (**1B**) | Triplet 4-nitrene-4′-nitrostilbene (**2B**) |
|---|---|---|
| 80 | $7.865\times10^{-4}$ | $1.66\times10^{-4}$ |
| 82 | $1.966\times10^{-3}$ | – |
| 84 | $5.932\times10^{-3}$ | $1.48\times10^{-3}$ |
| 85 | $1.172\times10^{-2}$ | – |
| 87 | – | $9.43\times10^{-3}$ |
| 89 | – | $2.14\times10^{-2}$ |

[a]Experimental error, ±0.0003 min$^{-1}$.

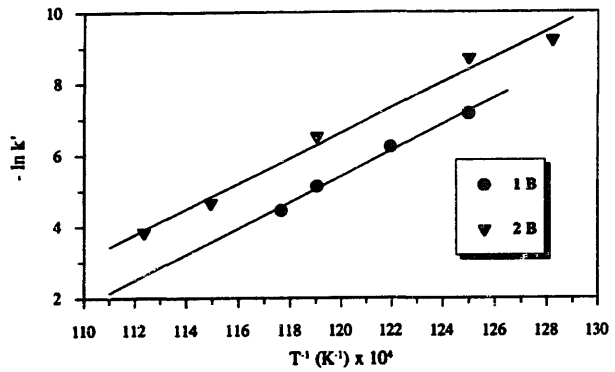


Fig. 6. Plot of the logarithmic rate constants ($\ln k'$) of the thermal hydrogen abstraction of **1B** and **2B** between 77 and 90 K in 2-MTHF vs. $1/T$ according to the Arrhenius equation. The lines show the least-squares linear regression slopes.

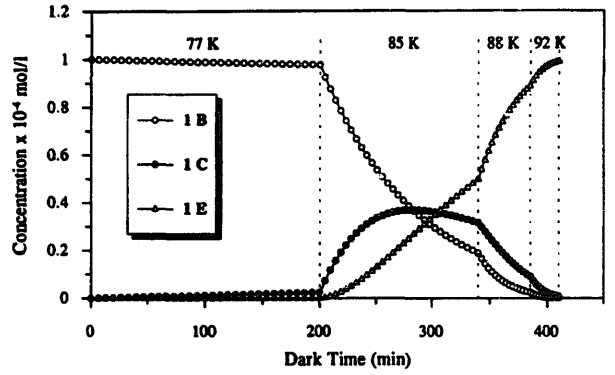


Fig. 7. Simulation of the concentration–time functions of **1B**, **1C** and **1E** during the thermal reaction shown in Fig. 1d (for further details, see text).

mined by the ratio of the rate constants for both steps. This means that only a stationary concentration of the imino radical is available experimentally, which makes it difficult to obtain kinetic information about its thermal reaction. In contrast to the thermal reaction, the photochemical reaction of triplet 4-nitrophenylnitrene (**1B**) quickly leads to the nearly quantitative formation of the imino radical **1C** (Fig. 1b). This allows investigation of the kinetic behavior of the thermal hydrogen abstraction of **1C**.

Since 4-nitroaniline (the product of the thermal reaction of the imino radical) and the imino radical absorb in the same spectral region (Fig. 1c), only global information about the thermal reaction of **1C** is available from the UV-Vis experiments (no rate constants). It follows from a comparison of the experiments shown in Fig. 1c and 1d that similar amounts of the imino radical and the nitrene require a similar amount of time (about 7 h) for their thermal reaction (at similar temperatures) to form **1E**. This implies that the activation energy of both abstraction steps is in the same order of magnitude. On the basis of these arguments, the concentration–time functions (**1B**, **1C** and **1E**) of the thermal reaction, shown in Fig. 1d, are simulated in Fig. 7 ($k'_1 = k'_2$ is assumed). As demonstrated in Fig. 7, the UV-Vis spectra of the products shown in Fig. 1d are a superimposition of those of **1C** and **1E**. Species **1C** is dominant up to about 300 min and **1E** is dominant above 350 min of the dark reaction under the given conditions.

Beside the hydrogen abstraction, no other significant bimolecular thermal reactions of the nitrenes were observed between 77 and 86 K in 2-MTHF. To explain this finding, the activation energy that is required for diffusion ($E_D$) in a solid 2-MTHF glass was estimated on the basis of the temperature-dependent dynamic viscosity measured by Ling and Willard [14]. Using these values, temperature-dependent diffusion coefficients were calculated according to the Einstein–Stokes equation

$$D = \frac{kT}{6\pi r\eta}$$

where $k$ is the Boltzmann constant, $T$ is the temperature, $r$ is the radius of the molecules and $\eta$ is the dynamic viscosity at $T$. The activation energy $E_D$ was determined using the equation of the temperature dependence of the diffusion coefficient by plotting $\ln D$ vs. $1/T$ (Fig. 8).

$$D = D_0 e^{-\frac{E_D}{RT}}$$

where $D$ and $D_0$ are diffusion coefficients, $E_D$ is the activation energy required for diffusion, $R$ is the gas constant and $T$ is the temperature. The evaluation gives straight lines in all cases investigated (the regression coefficient was greater than 0.99). Assuming an active radius ($r$) of about 3 Å, an activation energy $E_D$ of 87 kJ mol$^{-1}$ was estimated in the solid 2-MTHF matrix ($E_D = 59$ kJ mol$^{-1}$ in 3-methylpentane (3-MP)). While the $E_D$ values for solutions are between 5 and 20 kJ mol$^{-1}$, the $E_D$ values for solids are between 150 and 500 kJ mol$^{-1}$ [15]. Since the glass state lies between these two states, the $E_D$ values determined for the organic glasses are very reliable.

The activation energy of the hydrogen abstraction of **1B** and **2B** was estimated to be about 30 kJ mol$^{-1}$, whereas diffusion in the solid 2-MTHF matrix requires a higher amount. This explains why the hydrogen abstraction is, under the given conditions, much more favored than bimolecular

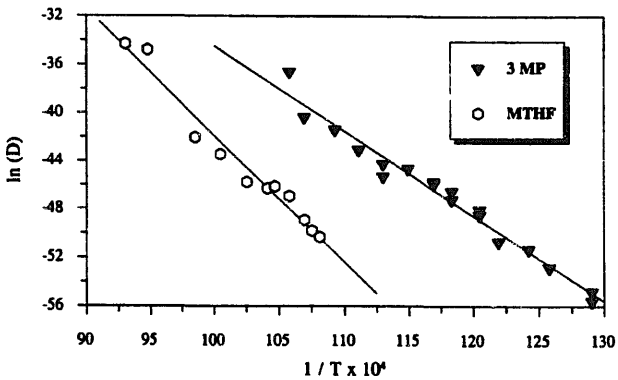


Fig. 8. Plot of the logarithmic temperature-dependent diffusion coefficients ($D$) of 2-methyltetrahydrofuran (2-MTHF) and 3-methylpentane (3 MP) vs. $1/T$ according to the Arrhenius equation. The $D$ values are calculated on the basis of the dynamic viscosity measured by Ling and Willard [14].

processes such as diazo coupling and others (e.g. the addition of triplet oxygen).

### 3.4. Mechanistic aspects of the optically induced hydrogen abstraction of nitrenes

In contrast to triplet 4-nitrophenylnitrene (**1B**), 4-nitrene-4'-nitrostilbene (**2B**) does not efficiently abstract hydrogen after photochemical excitation. The UV-Vis spectra of **1B** and **2B** indicate that the energy difference between the ground and electronically excited states is lower for the stilbenenitrene than for the phenylnitrene.

From the present point of view, the findings can be explained by two models: (a) by a hydrogen abstraction starting from a hot ground state of the nitrene (produced indirectly by an ic process); and (b) by a hydrogen abstraction starting from an electronically excited state.

(a) With regard to the fact that we have not observed any emission from both triplet 4-nitrophenylnitrene and triplet 4-nitrene-4'-nitrostilbene, it can be plausibly assumed that the deactivation of their excited states proceeds mainly by radiationless processes (ic). The released energy is vibrational energy. It is dissipated over the nitrene skeleton, partially resulting in an increase in temperature but also in a transfer of vibrational momentum and energy to the solvent molecules which are present in the surroundings of the relaxing nitrene. If the energy content of the nitrene–solvent system is high enough, the activation barrier of the hydrogen abstraction is passed and the reaction is efficient. This is realized in phenylnitrene (**1B**: $\lambda_{max} = 312$ nm) derivatives but obviously not in stilbenenitrenes (**2B**: $\lambda_{max} = 450$ nm) and in related molecules which absorb at longer wavelengths.

(b) As mentioned before, the energy of the excited triplet states of **1B** and **2B** differs. The excitation energy of **1B** is much higher than that of **2B**. The reaction enthalpy of the hydrogen abstraction of the excited **1B** should therefore be more exergonic than in the case of the hypothetical abstraction reaction of the excited **2B**. On the basis of the Bell–Evans–Polanyi principle [17], it follows that the activation barrier of the hydrogen abstraction by the excited **2B** is higher than that by the excited **1B**. This difference in the activation energies also explains the experimental finding that at 77 K the excited **1B** reacts with the matrix solvent whereas **2B** is stable on excitation.

A decision as to which model is valid cannot be taken on the basis of the current experimental results.

### 3.5. MO calculations regarding the hydrogen abstraction of arylnitrenes

We were interested in the investigation of the primary hydrogen abstraction of triplet nitrenes using MO methods because of the outstanding importance of this reaction amongst their deactivation processes.

The thermal hydrogen abstraction starts from the triplet ground state ($T_1$) of the nitrenes **1B** and **2B**, whereas it is not clarified experimentally whether the photochemically induced hydrogen abstraction of **1B** occurs on the "hot" $T_1$ (generated by ic deactivation of electronically excited states) or on the $T_2$ state. Nevertheless, we assume that the reaction runs from a "hot" electronic ground state $T_1$ not least owing to the probably small life-time of the $T_2$ state.

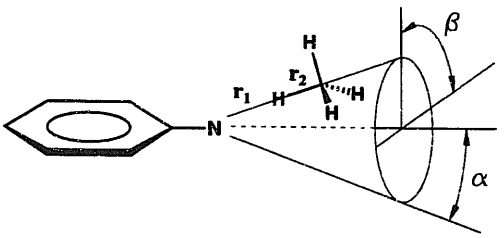


Fig. 9. Grid search of the system phenylnitrene–methane.

In the ground state, arylnitrenes have two singly occupied p orbitals. One is a p orbital which is in conjugation with the delocalized orbitals of the aromatic system, and the other is an in-plane p orbital [18]. Consequently, the hydrogen donator can attack the nitrene from two directions. To find the preferred direction, a grid search regarding the approximation of methane to phenylnitrene was performed on a semiempirical level (PM3, UHF) (semiempirical calculations were performed with the program MOPAC7 [19]). The 4-nitro group was omitted at the first step of optimization. Thus a methane molecule was moved around the nitrene nitrogen atom on a funnel surface with a constant distance $r_1 = 1.5$ Å. We varied the "funnel opening angle" $\alpha$ and the angle $\beta$ (Fig. 9).

The energy surface obtained and the corresponding contour plot is shown in Fig. 10.

From Fig. 10, it follows that the energy is lowered if the methane molecule lies on the surface of a funnel with $50° \leq \alpha \leq 55°$. The minimum is located in the plane of the aromatic ring ($\alpha = 55°$, $\beta = 0°$). Afterwards, the distances $r_1$ and $r_2$ were varied in order to find the saddle point. Starting with $r_1 = 1.22$ Å, $r_2 = 1.35$ Å, we performed a transition state optimization on increasing levels of theory. Finally we replaced the hydrogen atom in the 4-position of the UHF/6-31G* optimized transition state by a nitro group and repeated the optimization (ab initio calculations were performed with the program packet GAUSSIAN 92 [20]). The obtained transition state structure **3** is shown in Fig. 11. Some atoms are numbered in order to characterize the transition state geometry. The most important geometric parameters are listed in Table 2.

At this point, a comparison with the similar transition state of the system triplet formaldehyde–methane is useful. This transition state was found to be of earlier nature [21]. Although the direction of the attack and the analogous angles (see Table 2) are very similar, the positions of the transferred hydrogen atoms are clearly different. Thus, the C–H distance ($r$(1,2) in Fig. 11), calculated on the same level of theory, is more than 0.08 Å longer in the 4-nitrophenylnitrene–methane transition state. These findings suggest a later nature of the transition state **3** in comparison to Ref. [21].

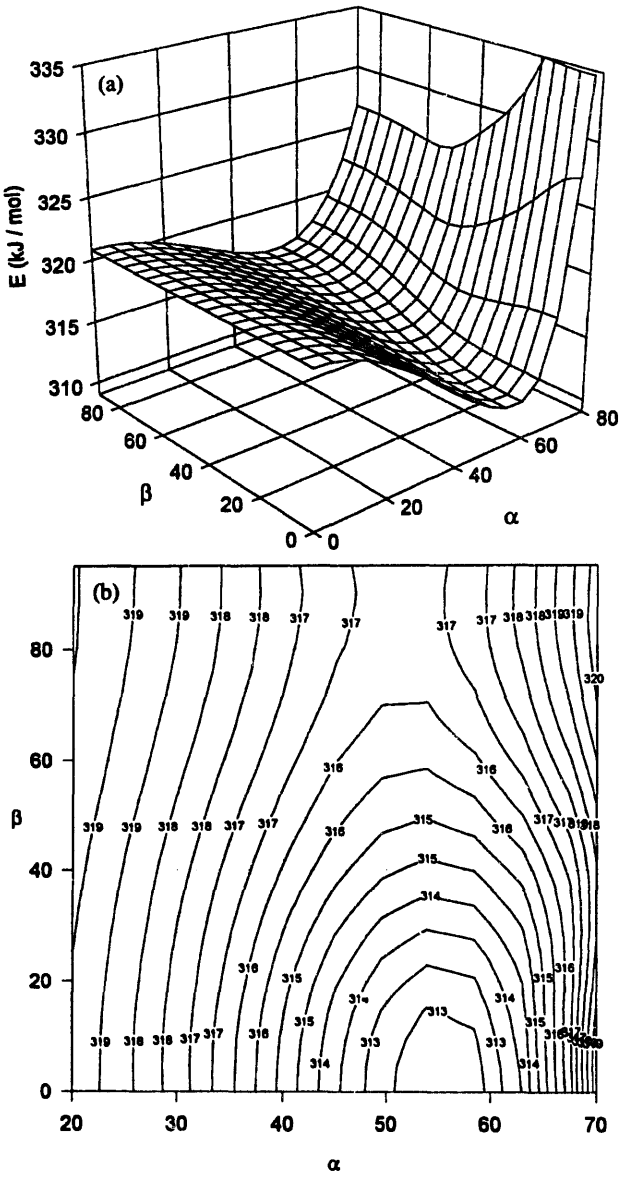


Fig. 10. Energy surface and contour plot of the system phenylnitrene–methane.

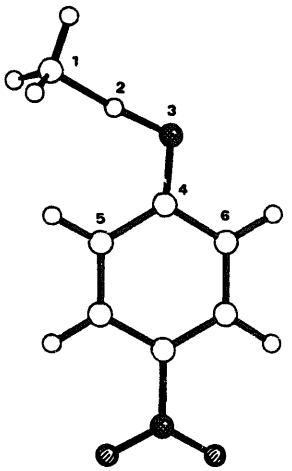

Fig. 11. Transition state structure of 4-nitrophenylnitrene–methane (3).

Table 2
Geometric parameters of the 4-nitrophenylnitrene- methane transition state

| Parameter | Value |
|---|---|
| $r$(1,2) (Å | 1.408 |
| $r$(2,3) (Å) | 1.226 |
| $r$(3,4) (Å) | 1.342 |
| $a$(1,2,3) (deg) | 175.4 |
| $a$(2,3,4) (deg) | 110.9 |
| $a$(3,4,5) (deg) | 125.3 |
| $a$(3,4,6) (deg) | 116.6 |
| $d$(1,2,3,4) (deg) | 180.0 |
| $d$(2,3,4,5) (deg) | 0.1 |

Fig. 12. The $C_s$ symmetric phenylimino radical (4).

In spite of the fact that a transition state with an "orthogonal" attack of the methane molecule could not be found, it was checked whether only one stable conformer of the imino radical exists. Optimization of the non-planar $C_s$ symmetric phenylimino radical (4) both on the ROHF/6-31G* and the MCSCF/6-31G* level was therefore performed. The subsequent vibrational analysis proved that the energy of 4 has no energy minimum but that 4 is a transition state on the energy hypersurface. This means that there is no activation barrier between the orthogonal state 4 and the energetically favored planar state of the imino radical. From these energy arguments, it follows that 4, if formed, has a very short lifetime (see Fig. 12).

## Acknowledgements

The financial support of the micro resist technology GmbH (Berlin) and of the Deutsche Forschungsgemeinschaft (Bonn) is gratefully acknowledged. The authors also thank Ms. Katrin Harder for proof reading this paper.

## References

[1] E. Leyva, M.S. Platz, G. Persy and J. Wirz, *J. Am. Chem. Soc., 108* (1986) 3783.
[2] (a) O.L. Chapman and J.-P. Le Roux, *J. Am. Chem. Soc., 100* (1978) 282. (b) O.L. Chapman, R.S. Sheridan and J.-P. Le Roux, *J. Am. Chem. Soc., 100* (1978) 6245.
[3] J.C. Hayes and R.S. Sheridan, *J. Am. Chem. Soc., 112* (1990) 5879.
[4] (a) J. Bendig, R. Mitzner and L. Dähne, Makromol. Chem., *Macromol. Symp., 18* (1988) 145. (b) L. Dähne, J. Bendig and R. Stößer, *J. Prakt. Chem., 334* (1992) 707.
[5] H. Bayley, *Lab. Tech. Biochem. Mol. Biol.*, (1983) 12.
[6] T.-Y. Liang and G.B. Schuster, *J. Am. Chem. Soc., 109* (1987) 7803.
[7] S.P. Efimov, V.A. Smirnov and A.V. Pochinok, *Chimija Vysokich Energij, 17*(1) (1983) 445.
[8] V.A. Smirnov and S.B. Brichkin, *Chem. Phys. Lett., 87*(6) (1982) 548.

[9] I.R. Dunkin, private communication [6].
[10] T. Harder, J. Bendig, G. Scholz and R. Stößer, *J. Am. Chem. Soc., 118* (1996) 2497.
[11] E. Leyva, M.J.T. Young and M. Platz, *J. Am. Chem. Soc., 108* (1986) 8307.
[12] E. Leyva, D. Munoz and M.S. Platz, *J. Org. Chem., 54* (1989) 5938.
[13] K. Kanakarajan, R. Goodrich, M.J.T. Young, S. Soundararajan and M.S. Platz, *J. Am. Chem. Soc., 110* (1988) 6536.
[14] (a) A.C. Ling and J.E. Willard, *J. Phys. Chem., 72* (1968) 1918. (b) T. Harder, J. Bendig, G. Scholz and R. Stößer, *J. Inf. Rec. Mat., 23* (1996) 147.
[15] H.-D. Jakubke and H. Jeschkeit, *Lexikon der Chemie*, F.A. Brockhaus Verlag, Leipzig, 1987, p. 281.
[16] M.E.C. Biffin, J. Miller and D.B. Paul, in *The Chemistry of the Azido Group*, Interscience, London, 1971, p. 57.
[17] M.I.S. Dewar, *The Molecular Orbital Theory of Organic Chemistry*, McGraw-Hill, New York, 1969.
[18] R. Liu and X. Zhou, *Chem. Phys. Lett., 207* (1993) 185.
[19] Frank J. Seiler, MOPAC7 Program, Res. Lab., U.S. Air Force Academy, Colorado Springs, CO, 1995.
[20] M.J. Frisch, G.W. Trucks, M. Head-Gordon, P.M.W. Gill, M.W. Wong, J.B. Foresman, B.G. Johnson, H.B. Schlegel, M.A. Robb, E.S. Replogle, R. Gomperts, J.L. Andres, K. Raghavachari, J. S. Binkley, C. Gonzalez, R.L. Martin, D.J. Fox, D.J. Defrees, J. Baker, J.J.P. Stewart and J.A. Pople, GAUSSIAN 92, Revision G.2, Gaussian, Inc., Pittsburgh PA, 1992.
[21] A.E. Dorigo, M.E. McCarrick, R.J. Loncharich and K.N. Houk, *J. Am. Chem. Soc., 112* (1990) 7508.